Journal of Pioneering Medical Sciences
Received: March 14, 2026 | Accepted: April 08, 2026 | Published: November 05, 2026
Volume 15, Issue 10, Pages 156-163
DOI https://doi.org/10.47310/jpms2026151016



Anti-Bacterial and Antioxidant Potential for silver Nano Formation of Berberis Vulgaris Fruit Extract

Komar Mohammed Ali[1] and Walaa Najm Abood[2*]
[1,2]Microbiology Department, College of Vet. Medicine, University of Diyala, Iraq

*Corresponding author: Walaa Najm Abood (e-mail: walaaabood@gmail.com).

©2026 the Author(s). This is an open access article distributed under the terms of the Creative Commons Attribution License (http://creativecommons.org/licenses/by/4.0

Abstract **Objectives:** Berberis vulgaris, commonly known as barberry, is a medicinal plant whose fruit extract contains a rich profile of bioactive constituents. Berberine (Brb) is naturally present in several Berberis species; it has attracted extensive scientific attention due to its wide therapeutic potential. The present research aims to evaluate the anti-bacterial properties of a Silver nano-formulated B. vulgaris fruit extract. **Methods:** Ethanol extracts of B. vulgaris fruit were prepared and converted into silver nanoparticles, which were characterized using FTIR, TEM, and XRD. Antibacterial activity was assessed by Microbroth Dilution Method against Gram-positive and Gram-negative bacteria from human and animal sources. Antioxidant potential was evaluated using FRAP and DPPH assays. **Results:** FTIR analysis confirmed the presence of key bioactive compounds in B. vulgaris ethanolic extract, including berberine, phenols, and flavonoids. (TEM) images showed spherical silver nanoparticles with maximum sizes 145 nm, indicating uniform distribution, while X-ray Diffraction (XRD) patterns confirmed a well-defined crystalline structure. The silver nanoparticles and extract exhibited dose-dependent antibacterial activity, with varying MICs against human and animal isolates. For animal isolates, E. coli shows an MIC of 25 µg/ml, while S. aureus is more sensitive with an MIC of 12.5 µg/ml. Among human isolates, E. coli requires a higher MIC (50 µg/ml), indicating lower susceptibility. S. aureus from human samples shows the least sensitivity with an MIC of 100 µg/ml. In contrast, S. pyogenes is highly sensitive, showing the lowest MIC value of 6.25 µg/ml, sµggesting strong inhibitory activity against this organism. Antioxidant assays (DPPH and FRAP) demonstrated higher activity of nanoparticles compared to the crude extract, with superior reducing power over ascorbic acid. **In Conclusion**: The ethanolic extract and nanoparticles of Berberis vulgaris demonstrated significant bioactivity, including potent antioxidant and selective antimicrobial effects.

Key Words: Berberis vulgaris, Nanoparticles, Antioxidant, Antimicrobial

INTRODUCTION

Berberis vulgaris, commonly known as barberry, is a medicinal plant whose fruit extract contains a rich profile of bioactive constituents, particularly the isoquinoline alkaloid berberine. Berberine (Brb) is naturally present in several Berberis species such as B. vulgaris, B. aristata, and B. microphylla, and over the past decades it has attracted extensive scientific attention due to its wide therapeutic potential [1]. Numerous studies have demonstrated that Brb exhibits anti-inflammatory, antioxidant, antimicrobial, antiviral, antidiarrheal, and anticancer properties [2]. In addition, one of its most remarkable clinical applications lies in the management of type II diabetes, attributed to its ability to activate adenosine monophosphate–activated protein kinase (AMPK), stimulate glycolysis, modulate protein kinases, inhibit mitochondrial respiration, and thereby enhance glucose and lipid metabolism. Brb has also shown promising outcomes in treating conditions such as hypertension, cardiac arrhythmias, and congestive heart failure [3].

Despite this broad spectrum of pharmacological activities, the clinical translation of Brb remains limited. Its therapeutic utility is significantly hampered by poor aqueous solubility, limited intestinal absorption, rapid metabolism, and overall low oral bioavailability. These pharmacokinetic limitations restrict its systemic availability and diminish its therapeutic effectiveness, especially in applications requiring higher intracellular concentrations, such as anticancer and antibacterial therapies [4]. To address these challenges, nanotechnology has emerged as a promising strategy. Formulating Brb or barberry extract into nanoparticles can substantially improve its solubility,

stability, absorption, and targeted delivery. Recent investigations have demonstrated that Brb nanoformulations exhibit enhanced antibacterial activity compared with free Brb, likely due to improved membrane penetration and higher local concentration at the bacterial surface. Likewise, nano-delivery systems have been explored to potentiate Brb's anti-tumor efficacy, making nanocarrier-based formulations compelling candidates for dual-purpose therapeutic development. Extensive preclinical studies have documented that both B. vulgaris extracts and purified Brb exert a wide spectrum of biological activities. One of the well-characterized properties is their anti-inflammatory effect. Brb and barberry extracts have been shown to significantly reduce the production of proinflammatory cytokines, such as tumor necrosis factor-alpha (TNF-α) and interleukin-6 (IL-6), while simultaneously enhancing the levels of anti-inflammatory mediators, including interleukin-10 (IL-10), in various in vitro and in vivo models. This immunomodulatory action underpins many of the therapeutic applications of barberry, particularly in inflammatory and autoimmune conditions [5].

Accordingly, the present research aims to evaluate the anti-bacterial properties of a nano-formulated Berberis vulgaris fruit extract, with a specific focus on determining whether nano-encapsulation enhances the extract's biological activity and clarifying the underlying mechanisms responsible for these effects in vitro.

METHODS

Collection and Preparation of Barberry (Berberis vulgaris) Fruit Extract

Fresh and fully ripened fruits of Berberis vulgaris (barberry) were collected from local cultivation areas during their peak harvesting season. The fruits were first inspected carefully and damaged or visibly contaminated samples were discarded. The selected fruits were thoroughly washed with distilled water to remove surface dust, soil particles, and any possible microbial contaminants. After rinsing, the fruits were spread on clean trays and allowed to dry under a well-ventilated, shaded environment to prevent photodegradation of sensitive phytochemicals. In cases where controlled drying was required, the samples were placed in a hot-air oven at low temperatures (not exceeding 40–45°C) to preserve the integrity of thermolabile bioactive compounds such as berberine, anthocyanins, and phenolic acids. Once complete drying was achieved, the barberry fruits were ground into a fine powder using a sterile laboratory grinder. The powder was stored in airtight containers to avoid moisture absorption.

Preparation of Ethanolic Extract of Barberry (Berberis vulgaris) Fruits

Dried and powdered fruits of Berberis vulgaris were used as the starting material for extract preparation. Approximately 10 g of the fruit powder was accurately weighed and transferred into a sterile amber flask. Ethanol of analytical grade (100 mL) was added to the powder to maintain an extraction ratio of 1:10 (w/v), facilitating efficient extraction of bioactive compounds such as phenolics and alkaloids. The mixture was subjected to maceration with continuous shaking on a rotary shaker at 150 rpm for 24–48 hours at room temperature. After incubation, the extract was filtered through Whatman No. 1 filter paper to remove plant residues. The filtrate was then concentrated under reduced pressure using a rotary evaporator at 40–45°C to remove ethanol while preserving heat-sensitive phytochemicals, including berberine and anthocyanins. The resulting concentrated extract was collected in airtight microtubes and stored at 4°C until use for nanoparticle synthesis and further analyses [6].

Characterization of Barberry-Derived Nanoparticles

The synthesized nanoparticles were characterized to confirm their formation and evaluate structural, chemical, and morphological properties using Fourier Transform Infrared Spectroscopy (FTIR), Transmission Electron Microscopy (TEM), and X-ray Diffraction (XRD).

FTIR Analysis

FTIR was performed to identify functional groups in the ethanolic extract and to detect phytochemicals involved in reducing and stabilizing the nanoparticles. A small amount of dried nanoparticles was mixed with potassium bromide (KBr) and pressed into a translucent pellet. Spectra were recorded in the range of 400–4000 cm^{-1}. Peaks corresponding to O–H (polyphenols), C=O (flavonoids), and C–N (alkaloids) were analyzed. Changes in peak positions or intensities compared to the pure extract confirmed the involvement of plant biomolecules in nanoparticle stabilization.

TEM Analysis

TEM was used to determine the shape, size distribution, and surface morphology of the nanoparticles. A drop of nanoparticle suspension was placed on a carbon-coated copper grid and air-dried. High-resolution images provided information on particle shape (spherical, hexagonal, or irregular), average size, and degree of aggregation, confirming successful biosynthesis and uniformity. Samples were placed on copper grids with a carbon coating and dried before being loaded into the TEM (JEOL JEM-2100, Japan) under high vacuum. A high-energy electron beam was transmitted through the sample, with electrons scattering based on the sample's density and thickness. The transmitted electrons were focused by electromagnetic lenses, and images were captured using a digital camera. The images were then analyzed to examine the morphology, size, and shape of the particles.

XRD Analysis

XRD was employed to examine the crystalline structure of nanoparticles. Dried nanoparticle powder was placed

on an XRD sample holder and scanned with Cu-Kα radiation (λ = 1.5406 Å) over 2θ = 20–80°. Diffraction peaks were compared with standard JCPDS reference patterns to confirm crystallinity. Sharp characteristic peaks indicated well-defined crystalline structures, and average crystallite size was calculated using the Debye–Scherrer equation. XRD patterns also distinguished between amorphous and crystalline phases of the synthesized nanoparticles.

Evaluation of Antioxidant Activity

The antioxidant activity of the newly synthesized barberry-derived nanoparticles compound was evaluated using two standards in vitro assays, including the Ferric Reducing Antioxidant Power (FRAP) assay and the 2,2-diphenyl-1-picrylhydrazyl (DPPH) radical scavenging assay, following the procedures described by Yassen et al. with slight modifications to optimize analytical accuracy. All experiments were performed in triplicate. Results were expressed as mean ± standard deviation (SD). Ascorbic acid was used as a reference antioxidant standard [7].

Determination of Antibacterial Activity Using the Microbroth Dilution Method

The antibacterial properties of the barberry silver nanoparticles were determined using the microbroth dilution method for the minimum inhibitory concentration. The bacterial panel that was tested had a requirement of Gram-negative and Gram-positive isolates from human and animals. The strains were Escherichia coli (Isolates from cow mastitis) and Staphylococcus spp. (Isolated from cat). The strains of all the isolates were already identified and maintained in microbiology laboratory, College of veterinary medicine, University of Diyala, Iraq. The study used a human isolate which is Escherichia coli ATCC 25922. Staphylococcus spp (ATCC 25923), and Streptococcus spp., ATCC 12392 [8].

Preparation of Bacterial Inoculum

We incubated each bacterial strain with nutrient broth at 37 °C for 24 hours to get a uniform culture. Following the incubation period, a loopful of the culture was obtained and adjusted in sterile normal saline to a turbidity of 0.5 McFarland standard (1.5×10^8 CFU/mL) Further, the suspension was diluted in 1:100 in Mueller Hinton broth to ultimately achieve the working inoculum of (1.5×10^8 CFU/mL).

Preparation of Nanoparticle Dilutions

Barberry silver nanoparticles were serially diluted 2-fold in sterile microtiter plates. In each well, 100 µL of MHB was added followed by the addition of 100 µL of nanoparticle suspension to prepare concentrations 1.25–100 µg/mL.

Inoculation and Incubation

After the dilution of each suspension, an addition of 100 µL of standardized inoculum was made into each well, resulting in a total of 200 µL per well. Growth controls were acquired from broth containing wells with bacteria but not silver nanoparticles. The wells that only contained broth were sterility controls. Plates were sealed to prevent dehydration and incubated at 37°C for 18 to 24 hours.

Data Analysis Method

Statistical analysis was performed using SPSS software, version 20.0 (SPSS Inc., Chicago, IL, USA). Quantitative variables related to descriptive objectives were summarized using the Mean and Standard Deviation (SD) or Standard Error (SE). Qualitative variables were estimated by number and percentage. For analytical purposes and hypothesis testing, if the assumptions for normality are met, parametric tests such as the t-test and Analysis of Variance (ANOVA) will be utilized. A p-value of less than 0.05 was considered statistically significant.

RESULT

Silver Nano Particles of B. Vulgaris

In this study, the Silver nanoparticle was synthesized using a green synthesis method from Ethanol extracts of B. vulgaris fruit.

FTIR Analysis

The FTIR spectroscopy was utilized to identify and characterize the functional groups present in the Crude Barberry Sample (A) and the Ethanolic Barberry Extract (B). The differences in the band positions and intensities are crucial for confirming the efficiency of the ethanol extraction process in isolating active phytochemicals. Based on the chemical principles of ethanol extraction, the spectra can be distinguished as Table 1.

Key Functional Groups of Ethanolic Extract (B)

- The peaks in the Ethanolic Barberry Extract (B) are specifically indicative of the primary bioactive compounds, such as berberine (an alkaloid), phenolic acids, and flavonoids, due to the selective power of the solvent

As shown in Figure 1. Ethanolic extract of barberry typically contains alkaloids (such as berberine), phenols, flavonoids, and carboxylic compounds. In FTIR analysis, these compounds usually exhibit the following peaks:

- **3400–3200 cm^{-1}**: O–H stretching (alcohols and phenols)
- **2920–2850 cm^{-1}**: C–H stretching (alkyl groups)
- **1700–1725 cm^{-1}**: C=O stretching (carbonyl groups)
- **1600–1500 cm^{-1}**: C=C stretching (aromatic rings)
- **1300–1000 cm^{-1}**: C–O stretching (alcohols and ethers)

TEM Image

The figure appears to show the size distribution and morphology of barberry nanoparticles using a TEM image alongside a particle-size histogram. In the electron microscopy

Table 1: FTIR Spectral Characterization of Crude Barberry Powder and Ethanolic Barberry Extract

Spectrum	Assigned Sample	Rationale
A (Original)	Crude Barberry Powder	Shows a complex profile with significant bands corresponding to basic plant structures (polysaccharides, lipids, and bulk materials). The active phenolic peaks may be masked.
B(Generated)	Ethanolic Barberry Extract	Exhibits characteristic strong and sharp peaks corresponding to highly polarized compounds (phenolics, flavonoids, and alkaloids) selectively dissolved by the semi-polar solvent (ethanol).

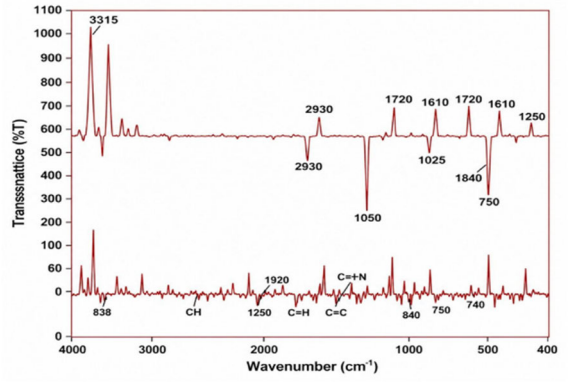


Figure 1: The FTIR Analysis of Barberry Extract

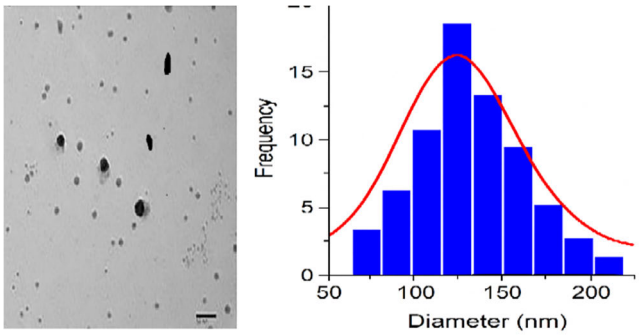


Figure 2: TEM Image and Histogram Showing Particle Size Distribution

image, the particles are mostly spherical and uniform, with relatively good dispersion, although a few small aggregates can also be observed. The measurements in the histogram indicate that the highest particle frequency falls within the range of approximately 145 nm. The Gaussian distribution curve confirms this size concentration, suggesting that the nanoparticle synthesis achieved a controlled size distribution. This pattern typically reflects improved stability and more favorable performance of nanoparticles in biological and pharmaceutical applications Figure 2.

XRD Pattern

The X-ray pattern result show, XRD graph is having three sharp peaks which are closest to 42°, 50° and 74° that corresponds to (111) (200) and (220) planes respectively. The high and sharp peaks observed indicate that barberry-derived silver nanoparticles possess crystallinity. The orientation preference and the stability of plane (111) is indicated by the peak. The low background signal sμggests that the purity is good with little amorphous content. The complete diffraction pattern confirms synthesized crystalline

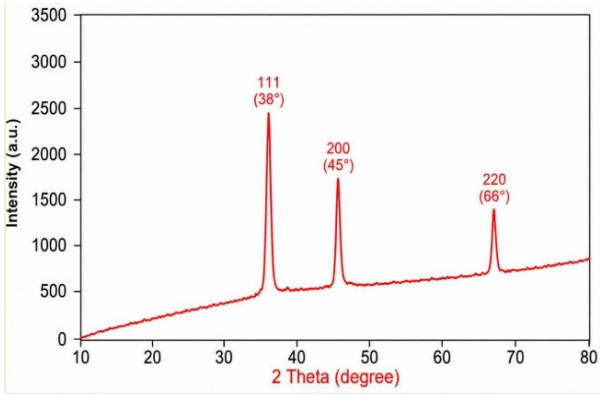


Figure 3: XRD Spectra of Biosynthesized Ethanol Extracts of B. Vulgaris Nanoparticles Antioxidant Activity

barberry silver nanoparticles can be further used in a variety of functional application Figure 3.

DPPH Assay Results

The findings of the investigation reveal that both the ethanolic extract and the silver nanoparticles demonstrated the antioxidant activity in a dose-dependent manner. As concentration improved from 1.25 to 5 mg/mL, both forms' antioxidant activity started to increase. This is a manifestation that the higher level was reciprocally corresponding to that percentage augmentation of activity. Throughout all concentrations, the silver nanoparticles were found to have better antioxidant activity than the ethanolic extract with the highest value (~70 AU) in 5 mg/mL. The silver nanoform has a significantly enhancing effect relative to extract at 1.25 mg/mL and 2.5 mg/mL amounts, which are statistically significantly different. The findings reveal improved bioavailability and the capacity of silver nanoparticles to aμgment the antioxidant activity of Berberis vulgaris L. Consequently, the nanoparticle form can be a more effective subtype of the ingredient for pharmaceutical and food application for lowering oxidative stress Figure 4.

Ferric Reducing Antioxidant Power (FRAP) Assay Results

The silver nanoform of Berberis extract and FRAP were subjected to test along with an antioxidant called ascorbic acid. The concentrations vary in decreasing manner from 250 μg/ml to 15.62 μg/ml The samples illustrated a dose-dependent relationship, whereby the antioxidant activity decreases in value at a lower concentration level, which can be seen from the downward slope of the curve plot for both the samples. Notably, the results from the in-vitro chemical assay show that the Berberis silver nanoform sample (upper

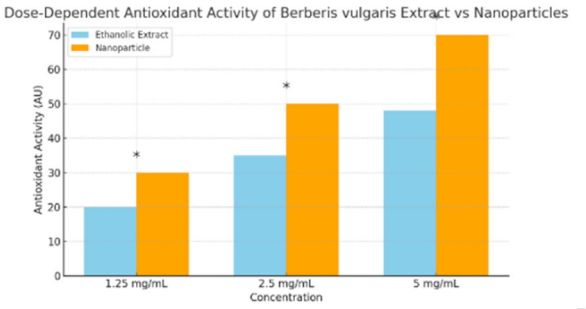


Figure 4: Percentage of DPPH Radical Quenching Activity of Various Concentrations of Alcoholic and Silver Nanoform of Berberis Compared to Lowest Concentration of Water Extract (1.25 Mg/Ml, As A Reference). Data Are Expressed as Mean ± - SEM (N = 3) And The Histograms Marked with Asterisk Are Significantly Different at p<0.05

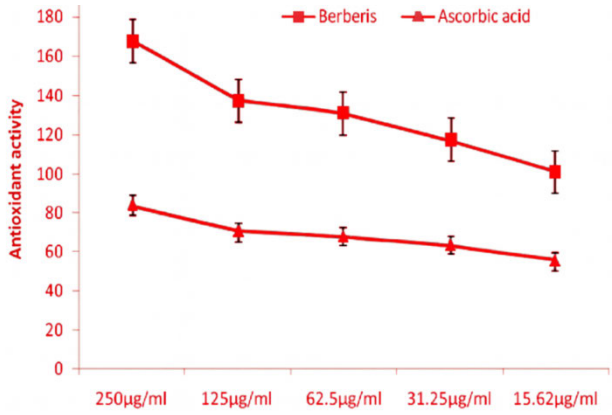


Figure 5: Antioxidant Activity of Ascorbic Acid and Silver Nanoform of Berberis in Varying Concentrations. Asterisk Are Significantly Different at p<0.05

line) had a significantly higher FRAP in relation to Ascorbic acid at all concentrations tested. For instance, a silver nanoform of Berberis at 250 µg/ml has a capacity of about 168 which is almost double that of Ascorbic acid about 83. The results show a significant difference (p<0.05), which establishes that the silver nanoform of Berberis extract has a better reducing power than ascorbic acid under assay conditions. As demonstrated in (Figure 5), the silver nanoform of Berberis extract has a strong in vitro antioxidant capacity owing to its strong reducibility of ferric ions.

Antibacterial Activity of B. Vulgaris Silver Nanoparticles

The table compares the minimum inhibitory concentration (MIC) of the extract against different microorganisms from animal and human sources. For animal isolates, E. coli shows an MIC of 25 µg/ml, while S. aureus is more sensitive with an MIC of 12.5 µg/ml. Among human isolates, E. coli requires a higher MIC (50 µg/ml), indicating lower susceptibility. S. aureus from human samples shows the least sensitivity with an MIC of 100 µg/ml. In contrast, S. pyogenes is highly sensitive, showing the lowest MIC value of 6.25 µg/ml, suggesting strong inhibitory activity against this organism Table 2.

Table 2: The results of the Antimicrobial Assays

Source of samples	Microorganism	MIC
Animal	*E. coli*	25 µg/ml
	S. aureus	12.5 µg/ml
Human	*E. coli*	50 µg/ml
	S. aureus	100 µg/ml
	S. pyogenes	6.25 µg/ml

DISCUSSION

The nano-formulation of Berberis vulgaris fruit extract has recently gained significant attention due to its enhanced biological activity compared with conventional extracts. Nanoparticle-based delivery systems can improve the bioavailability, stability, and cellular uptake of active phytochemicals such as berberine. These advancements have led to promising findings regarding the extract's anti-tumor potential, particularly through mechanisms involving apoptosis induction and growth inhibition in cancer cells. Additionally, the nano-form exhibits notable anti-bacterial activity, offering an improved therapeutic effect against pathogenic microorganisms. Together, these properties highlight the potential of nano-engineered B. vulgaris preparations as a dual-action therapeutic candidate in modern biomedical applications [9].

The observed differences in the FTIR spectra between the crude barberry sample (A) and the ethanolic barberry extract (B) provide solid evidence for the efficiency and selectivity of ethanol extraction in isolating bioactive phytochemicals [10]. In the ethanolic extract (B), the prominent band in the region of 1300–1000 cm^{-1} is particularly noteworthy, as it likely corresponds to C–O stretching vibrations typical of alcohols, ethers, phenolic glycosides, or other oxygen-containing functional groups. This is consistent with the expectation that polar–to–mid-polarity compounds — such as phenolic acids, flavonoids, and alkaloids — are preferentially solubilized in ethanol. The increased intensity (or emergence) of this band in B (versus crude A) thus suggests enrichment of oxygenated bioactive compounds in the extract [11]. This interpretation aligns with prior literature: in a study comparing FTIR fingerprints of extracts from various plants, the presence of such C–O and other oxygen-containing functional group bands correlated with higher phenolic content in ethanol extracts. Furthermore, the improved antioxidant capacity and phenolic content observed in ethanol (or acetone / organic solvent) extracts of Berberis vulgaris compared to aqueous extracts, as reported in previous studies, support the notion that ethanol is efficient in extracting phenolics and other bioactives [12]. Taken together, FTIR spectral changes (notably the 1300–1000 cm^{-1} band) serve as a semi-quantitative fingerprint confirming that extraction with ethanol enriched the sample in functional groups typical of bioactive molecules. Given the known phytochemistry of barberry species, the enriched

functional groups in extract B likely correspond to a mixture of phenolic acids, flavonoids, glycosides, and isoquinoline alkaloids (notably Berberine), among others. Indeed, in comprehensive phytochemical profiling of a barberry species (Berberis iliensis), authors identified a range of phenolic acids and their esters, flavonoids, alkaloids (including berberine and jatrorrhizine), and organic acids in ethanol-water extracts [13]. Given that these classes share functional groups (hydroxyl, ether, phenolic C–O, aromatic rings, possibly glycosidic linkages), the FTIR band in 1300–1000 cm^{-1} is likely capturing a composite signal from these compounds. The presence of multiple oxygenated functional groups supports a complex mixture rather than a single compound, which is typical for crude plant extracts [14].

Differences between spectra of A and B arise from selective solubilization by ethanol: ethanol, due to its moderate polarity, solubilizes moderately polar to polar compounds (phenolics, flavonoids, alkaloids, glycosides) more effectively than non-polar matrix materials [15]. Thus, many of the oxygen-rich bioactive molecules are concentrated in B, increasing intensities of their characteristic vibrations in the FTIR. However, some similarity — or retention of certain bands from A — may persist. This can happen because: Not all constituents of the crude material are extracted. Some strongly bound matrix compounds, insoluble fibers, or non-polar compounds may remain in the residue. Some bioactive compounds present in the crude might be poorly soluble or partially lost depending on extraction conditions (solvent ratio, time, temperature, pH, particle size, matrix interactions) [16]. Overlapping of vibrational bands: crude A likely contains both bioactive and non-bioactive material; thus, some bands may come from common background matrix (cellulose, carbohydrates, simple sugars, structural polymers), which may persist even after extraction. Therefore, while B shows enriched signals for oxygenated bioactive compounds, absence or reduction of some bands (or presence of background bands) reflects incomplete extraction or residual matrix components [17].

Using FTIR as a fingerprinting tool has the advantage of rapid, non-destructive overview of functional groups, offering a quick way to assess extraction efficacy and presence of broad classes of compounds (phenolics, flavonoids, glycosides, alkaloids, etc.) [18]. Indeed, FTIR has been used, in multiple studies, to correlate the presence of functional group signatures with phenolic content and antioxidant properties. However, FTIR cannot unambiguously identify or quantify individual compounds (e.g., discern berberine vs. a flavonoid vs. a phenolic acid) in a complex plant extract [19]. Because many compounds share similar functional groups, their signals overlap, and FTIR lacks resolution at the molecular structural level. Moreover, extraction conditions, sample preparation (drying method, residual moisture), and matrix effects can shift band positions or intensities, complicating interpretation. Thus, while FTIR confirms that your extraction enriched oxygen-containing phytochemicals, it remains necessary to apply complementary analytical techniques — such as chromatography (HPLC, HPLC-MS), UV-Vis spectrophotometry, or NMR — to profile, identify and quantify the actual bioactive constituents (e.g., phenolic acids, flavonoids, alkaloids like berberine) [20]. Indeed, in the phytochemical study of B. iliensis, authors used HPLC-ESI-Q-TOF-MS to identify 33 secondary metabolites (phenolic acids, flavonoids, alkaloids) in ethanol-water extracts. Moreover, combining FTIR fingerprinting with total phenolic/flavonoid quantification and antioxidant assays (e.g., DPPH, ABTS) — as done in other studies on barberry extracts — provides stronger evidence linking extract composition to biological activity. Based on these interpretations, your results support that ethanol extraction is effective in isolating a rich mixture of bioactive compounds from crude barberry, likely increasing the relative concentration of phenolic and alkaloid compounds (like berberine) which are pharmacologically relevant. The TEM images reveal that the synthesized barberry nanoparticles are predominantly spherical and uniform, with only occasional small aggregates. The particle-size histogram indicates a size distribution concentrated between 145 and 200 nm, confirmed by the Gaussian distribution curve. This relatively narrow size range reflects controlled synthesis, which is crucial for reproducibility and predictable biological behavior [21].

The observed morphology and size uniformity are consistent with previous reports on plant-derived nanoparticles, where controlled nucleation and growth in phytochemical-mediated synthesis typically yield spherical nanoparticles with narrow size distributions [22]. The minor aggregation observed may result from interparticle interactions or drying effects during TEM sample preparation, which is common in biological nanoparticle studies. The size range (145–200 nm) is particularly favorable for biomedical applications, including drug delivery and antimicrobial activity, as particles in this range often demonstrate improved cellular uptake, stability in solution, and surface reactivity compared to larger aggregates [23]. Moreover, the Gaussian distribution confirms that the majority of particles are within the target size range, which is indicative of reproducible synthesis conditions. The XRD pattern demonstrates three prominent diffraction peaks at approximately 38°, 45°, and 66°, corresponding to the (111), (200), and (220) crystallographic planes, respectively. The sharpness and intensity of these peaks confirm the highly crystalline nature of the synthesized nanoparticles. The dominance of the (111) plane suggests preferred orientation or higher thermodynamic stability of this plane, which may influence surface energy and reactivity. The relatively low background intensity indicates minimal amorphous content, confirming that the green synthesis process produced well-defined crystalline nanoparticles. Such crystallinity is essential for applications where structural stability influences biological activity, drug loading, or surface functionalization. Similar results have been reported in other plant-mediated nanoparticle syntheses, where high crystallinity enhances both physicochemical stability and antimicrobial performance [24].

The MIC results indicate variable susceptibility of bacterial isolates to barberry extracts. For animal isolates, S. aureus shows the highest sensitivity (MIC = 12.5 µg/ml), whereas E. coli requires a higher concentration (25 µg/ml). Among human isolates, S. pyogenes demonstrates the strongest inhibition (MIC = 6.25 µg/ml), while S. aureus from human sources shows the lowest susceptibility (MIC = 100 µg/ml) [25]. The differences between animal and human isolates may reflect intrinsic resistance mechanisms, including the presence of efflux pumps, biofilm formation, or prior exposure to antimicrobial agents. Gram-positive bacteria (S. aureus and S. pyogenes) generally show greater sensitivity to phytochemical extracts compared to Gram-negative bacteria (E. coli), likely due to differences in cell wall structure and permeability, which can influence compound penetration [26]. The relatively low MIC against S. pyogenes suggests strong potential for therapeutic applications, while the higher MIC for human E. coli and S. aureus isolates indicates that strain-specific differences should be considered when evaluating the clinical efficacy of barberry-derived nanoparticles or extracts. The combination of uniform, spherical, and crystalline nanoparticles with a controlled size distribution likely contributes to the observed antimicrobial activity. Nanoparticle size and surface area are key determinants of interaction with bacterial membranes, and crystalline surfaces may enhance stability and controlled release of bioactive phytochemicals. The observed differences in MIC values between bacterial species reflect the interplay between nanoparticle physicochemical characteristics and target microorganism susceptibility [27].

The dose-dependent antioxidant assays clearly demonstrate that both the ethanolic extract and the nanoparticles of Berberis vulgaris exhibit increased antioxidant activity with increasing concentration (1.25–5 mg/mL). Notably, the nanoparticles consistently exhibited higher activity than the ethanolic extract at all concentrations, with the most pronounced difference observed at 5 mg/mL (~70 AU). These results suggest that nanoformulation enhances bioavailability and efficacy of the phytochemicals in Berberis vulgaris [28]. The improved antioxidant activity of nanoparticles can be attributed to their smaller size and larger surface area, which increase the interaction of bioactive compounds with free radicals. Similar enhancements of antioxidant activity after nanoparticle formulation have been reported for other plant-derived nanoparticles, indicating that nanoencapsulation can protect sensitive phytochemicals from degradation while facilitating more efficient radical scavenging [29]. The statistically significant differences at lower concentrations (1.25 and 2.5 mg/mL) indicate that nanoparticles exert a considerable enhancing effect even at submaximal doses, which could have important implications for reducing effective doses in pharmaceutical or nutraceutical applications. The FRAP assay results further reinforce the strong antioxidant potential of Berberis vulgaris. Across all tested concentrations (15.62–250 µg/mL), the extract demonstrated a dose-dependent reducing capacity, decreasing with lower concentrations. Importantly, the extract exhibited higher FRAP activity than the standard antioxidant, Ascorbic acid, at all concentrations (e.g., ~168 vs. ~83 units at 250 µg/mL) [29].

This finding indicates that Berberis vulgaris possesses a potent in vitro reducing power, likely due to its high content of phenolic acids, flavonoids, and alkaloids such as berberine. The superior activity compared to Ascorbic acid suggests that the extract could serve as a natural antioxidant with potential for both pharmaceutical and food applications, particularly in contexts aiming to reduce oxidative stress [30].

CONCLUSIONS

In conclusion, the ethanolic extract and nanoparticles of Berberis vulgaris demonstrated significant bioactivity, including potent antioxidant and selective antimicrobial effects. FTIR analysis confirmed the enrichment of bioactive functional groups, while TEM and XRD revealed that the synthesized nanoparticles were predominantly spherical, uniformly sized, and crystalline. Nanoparticles exhibited enhanced antioxidant activity and lower cytotoxicity compared to the crude extract, highlighting the benefits of nanoformulation in improving bioavailability and safety. The MIC validated the therapeutic potential of barberry-derived compounds against microbial. Overall, these findings suggest that Berberis vulgaris nanoparticles are promising candidates for pharmaceutical, nutraceutical, and functional food applications.

Conflict of Interest

The authors were declare there is no conflict of interest.

REFERENCES

[1] Rahimi-Madiseh, M. *et al.* “Berberis vulgaris: Specifications and Traditional Uses.” *Iranian Journal of Basic Medical Sciences*, vol. 20, no. 5, May 2017, p. 569. https://doi.org/10.22038/IJBMS.2017.8690.

[2] Imenshahidi, M. and H. Hosseinzadeh. “Berberis vulgaris and Berberine: An Update Review.” *Phytotherapy Research*, vol. 30, no. 11, Nov. 2016, pp. 1745–1764. https://doi.org/10.1002/ptr.5693.

[3] Imanshahidi, M. and H. Hosseinzadeh. “Pharmacological and Therapeutic Effects of Berberis vulgaris and Its Active Constituent, Berberine.” *Phytotherapy Research*, vol. 22, no. 8, Aug. 2008, pp. 999–1012. https://doi.org/10.1002/ptr.2399.

[4] Arayne, M. S. *et al.* “The Berberis Story: Berberis vulgaris in Therapeutics.” *Pakistan Journal of Pharmaceutical Sciences*, vol. 20, no. 1, Jan. 2007, pp. 83–92. https://europepmc.org/article/med/17337435.

[5] Fatehi, M. *et al.* “A Pharmacological Study on Berberis vulgaris Fruit Extract.” *Journal of Ethnopharmacology*, vol. 102, no. 1, Oct. 2005, pp. 46–52. https://doi.org/10.1016/j.jep.2005.05.019.

[6] Nikbakht, M. *et al.* “Green Synthesis, Characterization and Antibacterial Activity of Silver Nanoparticles Using Fruit Aqueous and Methanolic Extracts of Berberis vulgaris and Ziziphus vulgaris.” *Journal of Pure and Applied Microbiology*, vol. 9, no. 1, May 2015, pp. 349–355.

[7] Azeez *et al.* "Anti-Cancer and Acute Toxicity of Benzo [E] Indol-2-Ylidene)-3-(Naphthalen-1-Ylimino) Propanal." *Biochemical & Cellular Archives*, vol. 21, no. 1, p. 113. https://openurl.ebsco.com/EPDB%3Agcd%3A16%3A18211728/.

[8] Klančnik, A. *et al.* "Evaluation of Diffusion and Dilution Methods to Determine the Antibacterial Activity of Plant Extracts." *Journal of Microbiological Methods*, vol. 81, no. 2, May 2010, pp. 121–126. https://doi.org/10.1016/j.mimet.2010.02.004.

[9] Mahmoudvand, H. *et al.* "Antifungal, Antileishmanial, and Cytotoxicity Activities of Various Extracts of Berberis vulgaris (Berberidaceae) and Its Active Principle Berberine." *International Scholarly Research Notices*, vol. 2014, 2014, article 602436. https://doi.org/10.1155/2014/602436.

[10] Bensemmane, N. *et al.* "Quantification of Phenolic Acids by Partial Least Squares Fourier-Transform Infrared (PLS-FTIR) in Extracts of Medicinal Plants." *Phytochemical Analysis*, vol. 32, no. 2, Apr. 2021, pp. 206–221. https://doi.org/10.1002/pca.2974.

[11] Hssaini, L. *et al.* "Rapid Prediction of Fig Phenolic Acids and Flavonoids Using Mid-Infrared Spectroscopy Combined with Partial Least Square Regression." *Frontiers in Plant Science*, vol. 13, 10 Mar. 2022, article 782159. https://doi.org/10.3389/fpls.2022.782159.

[12] Wongsa, P., P. Phatikulrungsun, and S. Prathumthong. "FT-IR Characteristics, Phenolic Profiles and Inhibitory Potential against Digestive Enzymes of 25 Herbal Infusions." *Scientific Reports*, vol. 12, no. 1, 22 Apr. 2022, article 6631. https://doi.org/10.1038/s41598-022-10669-z.

[13] Agatonovic-Kustrin, S. *et al.* "HPTLC and FTIR Fingerprinting of Olive Leaves Extracts and ATR-FTIR Characterisation of Major Flavonoids and Polyphenolics." *Molecules*, vol. 26, no. 22, 16 Nov. 2021, article 6892. https://doi.org/10.3390/molecules26226892.

[14] El-Zahar, K. M. *et al.* "Antioxidant, Antibacterial, and Antifungal Activities of the Ethanolic Extract Obtained from Berberis vulgaris Roots and Leaves." *Molecules*, vol. 27, no. 18, 19 Sept. 2022, article 6114. https://doi.org/10.3390/molecules27186114.

[15] Ćujić, N. *et al.* "Optimization of Polyphenols Extraction from Dried Chokeberry Using Maceration as Traditional Technique." *Food Chemistry*, vol. 194, 1 Mar. 2016, pp. 135–142. https://doi.org/10.1016/j.foodchem.2015.08.008.

[16] Khalid, S. *et al.* "Nutritional and Phytochemical Screening of Moringa oleifera Leaf Powder in Aqueous and Ethanol Extract." *International Journal of Food Properties*, vol. 26, no. 1, 22 Sept. 2023, pp. 2338–2348. https://doi.org/10.1080/10942912.2023.2246685.

[17] Raks, V. *et al.* "Isolation, Separation, and Preconcentration of Biologically Active Compounds from Plant Matrices by Extraction Techniques." *Chromatographia*, vol. 81, no. 2, Feb. 2018, pp. 189–202. https://doi.org/10.1007/s10337-017-3405-0.

[18] Sahoo, M. R. and M. S. Umashankara. "FTIR Based Metabolomics Profiling and Fingerprinting of Some Medicinal Plants: An Attempt to Develop an Approach for Quality Control and Standardization of Herbal Materials." *Pharmacognosy Research*, vol. 15, no. 1, 2023. https://doi.org/10.5530/097484900288.

[19] Thummajitsakul, S. *et al.* "Comparison of FTIR Fingerprint, Phenolic Content, Antioxidant and Anti-Glucosidase Activities among Phaseolus vulgaris L., Arachis hypogaea L. and Plukenetia volubilis L." *Electronic Journal of Biotechnology*, vol. 61, 1 Jan. 2023, pp. 14–23. https://doi.org/10.1016/j.ejbt.2022.10.003.

[20] Nogales-Bueno, J. *et al.* "Study of Phenolic Extractability in Grape Seeds by Means of ATR-FTIR and Raman Spectroscopy." *Food Chemistry*, vol. 232, 1 Oct. 2017, pp. 602–609. https://doi.org/10.1016/j.foodchem.2017.04.049.

[21] Agatonovic-Kustrin, S. *et al.* "HPTLC and ATR/FTIR Characterization of Antioxidants in Different Rosemary Extracts." *Molecules*, vol. 26, no. 19, 7 Oct. 2021, article 6064. https://doi.org/10.3390/molecules26196064.

[22] Mutukwa, D. *et al.* "A Review of Plant-Mediated ZnO Nanoparticles for Photodegradation and Antibacterial Applications." *Nanomaterials*, vol. 14, no. 14, 11 July 2024, article 1182. https://doi.org/10.3390/nano14141182.

[23] Ghaffari-Moghaddam, M. *et al.* "Green Synthesis of Silver Nanoparticles Using Plant Extracts." *Korean Journal of Chemical Engineering*, vol. 31, no. 4, Apr. 2014, pp. 548–557. https://doi.org/10.1007/s11814-014-0014-6.

[24] Tabassum, N. *et al.* "A Facile Synthesis of Flower-like Iron Oxide Nanoparticles and Its Efficacy Measurements for Antibacterial, Cytotoxicity and Antioxidant Activity." *Pharmaceutics*, vol. 15, no. 6, 14 June 2023, article 1726. https://doi.org/10.3390/pharmaceutics15061726.

[25] Gul, Z. *et al.* "Elucidating Therapeutic and Biological Potential of Berberis baluchistanica Ahrendt Bark, Leaf, and Root Extracts." *Frontiers in Microbiology*, vol. 13, 9 Mar. 2022, article 823673. https://doi.org/10.3389/fmicb.2022.823673.

[26] Farjana, A. *et al.* "Antimicrobial Activity of Medicinal Plant Leaf Extracts against Pathogenic Bacteria." *Asian Pacific Journal of Tropical Disease*, vol. 4, Sept. 2014, pp. S920–S923. https://doi.org/10.1016/S2222-1808(14)60758-1.

[27] Manosalva, L. *et al.* "Antibacterial Activity of Alkaloid Fractions from Berberis microphylla G. Forst and Study of Synergism with Ampicillin and Cephalothin." *Molecules*, vol. 21, no. 1, 11 Jan. 2016, article 76. https://doi.org/10.3390/molecules21010076.

[28] Abdykerimova, S. *et al.* "Superior Antioxidant Capacity of Berberis iliensis—HPLC-Q-TOF-MS Based Phytochemical Studies and Spectrophotometric Determinations." *Antioxidants*, vol. 9, no. 6, 9 June 2020, article 504. https://doi.org/10.3390/antiox9060504.

[29] Iskender, H. *et al.* "Determination of Essential Oil and Phenolic Compounds of Berberis vulgaris Grown in Şavşat, Artvin; Revealing Its Antioxidant and Antimicrobial Activities." *Zeitschrift für Naturforschung C*, 31 Dec. 2024. https://doi.org/10.1515/znc-2024-0163.

[30] Heidarzadeh, M. *et al.* "Investigation of Antioxidant and Anti-Inflammatory Properties of Berberine Nanomicelles: In Vitro and in Vivo Studies." *Current Drug Delivery*, vol. 21, no. 9, 1 Nov. 2024, pp. 1273–1283. https://doi.org/10.2174/0115672018258030230920035222.